forests

MDPI

Article

OSCA Genes in *Liriodendron chinense*: Characterization, Evolution and Response to Abiotic Stress

Yongchao Ke [1,†], Mingyue Xu [1,†], Delight Hwarari [1], Baseer Ahmad [1], Rongxue Li [1], Yuanlin Guan [1], Jinhui Chen [2,*] and Liming Yang [1,*]

[1] College of Biology and the Environment, Nanjing Forestry University, Nanjing 210037, China
[2] Key Laboratory of Forest Genetics and Biotechnology of Ministry of Education of China, Co-Innovation Center for Sustainable Forestry in Southern China, Nanjing Forestry University, Nanjing 210037, China
* Correspondence: chenjh@njfu.edu.cn (J.C.); yangliming@njfu.edu.cn (L.Y.)
† These authors contributed equally to this work.

Abstract: The hyperosmolality-gated calcium-permeable channels (OSCA) play an imperative role in the plant response to environmental stresses. Moreover, their characteristics in the ornamental woody plant *Liriodendron chinense*, widely dispersed in the southern region of China, is yet to be elucidated. In the present study, 399 OSCA proteins were identified from 31 plant genomes, and comparative phylogenetic analysis revealed that *LchiOSCAs* gene family is closely related to the Magnolia *Cinnamomum kanehirae* OSCAs. In *L. chinense*, 11 *LchiOSCA* genes were identified and distributed across eight chromosomes. Additionally, phylogenetic analysis of *LchiOSCAs* exhibited a classification into four subfamilies based on the tree arrangement, similarity in the gene structures, and conserved motif numbers and order. Gene duplication investigations were biased towards the tandem duplication events, accounting for 36% (4/11) of the *LchiOSCA* gene family. The interspecies collinearity analysis revealed a closer relationship between the *L. chinense OSCAs* and the *P. trichocarpa OSCAs*. Analysis in promoter regions of the *LchiOSCAs* showed the presence of multiple phytohormones and stress responsive elements. Specifically, the ABA-responsive elements had the greatest representation. 3D protein structures of the modeled *L. chinense* OSCAs exhibited a high homology with the template structures, providing a better understanding of LchiOSCAs' functionality at the proteome level. The expression pattern analysis of *LchiOSCAs* based on the transcriptome data and qRT-PCR in *L. chinense* leaves showed differential responses to drought, cold, and heat stress at varying degrees. Specifically, *LchiOSCA2* and *LchiOSCA4* were highly expressed under the three abiotic stresses. This research will provide valuable resources and further the understanding of plant *OSCA* genes in *L. chinense* for agronomic breeding and bio-engineering purposes.

Keywords: *OSCA* genes; *Liriodendron chinense*; gene structure; abiotic stress responses

check for updates

Citation: Ke, Y.; Xu, M.; Hwarari, D.; Ahmad, B.; Li, R.; Guan, Y.; Chen, J.; Yang, L. *OSCA* Genes in *Liriodendron chinense*: Characterization, Evolution and Response to Abiotic Stress. *Forests* **2022**, *13*, 1835. https://doi.org/10.3390/f13111835

Academic Editor: Reiner Finkeldey

Received: 25 September 2022
Accepted: 31 October 2022
Published: 3 November 2022

Publisher's Note: MDPI stays neutral with regard to jurisdictional claims in published maps and institutional affiliations.

Copyright: © 2022 by the authors. Licensee MDPI, Basel, Switzerland. This article is an open access article distributed under the terms and conditions of the Creative Commons Attribution (CC BY) license (https://creativecommons.org/licenses/by/4.0/).

1. Introduction

The external environmental stresses including drought, high, and low temperatures affect plant growth and the developmental processes [1,2]. In recent years, due to global warming, extreme weather conditions have occurred more frequently, thus increasing the abiotic stress impact on plants. Nonetheless, plants have evolved a series of morphological, physiological, biochemical, and molecular mechanisms to adapt to and resist abiotic stresses, in order to maintain the normal physiological metabolism processes of plants [2,3]. Plants use numerous signaling pathways to sense, modify, and send signals in response to stress, as well as to activate or inhibit the expression of genes that respond to stress. External stresses usually disrupt the equilibrium of plants and ultimately interrupt the cell membrane system [4]. As secondary messengers, calcium can produce calcium signals when plants are exposed to external stimuli, which guide a series of physiological and biochemical reactions

of plant cells under stress [5]. Calcium channels mainly include calcium transporters and calcium pumps [6]. With further developments in research, many kinds of calcium channels have been found.

Among the numerous calcium channels, a special type of channel, the hyperosmolality-gated calcium-permeable channel (OSCA), was the first calcium channel found in plants that can sense external osmotic stress [7]. All the *OSCA* genes of *Arabidopsis thaliana* (*A. thaliana*) have the domain of an unknown function 221 (DUF221 domain) related to the plant stress response. The three-dimensional structure analysis of the proteins of the OSCA family members OSCA1.1, OSCA1.2, and OSCA3.1 by cryogenic electron microscopy showed that these channels have a high structural similarity and belong to a new class of mechanosensitive ion channels [8–10]. Advances in the whole genome sequencing of plants has led to the identification of: 15, 11, 13, and 17 *OSCA* gene family members in *A. thaliana* [7], *Oryza sativa* (*O. sativa*) [11], *Vigna radiata* (*V. radiata*) [12], and *Populus trichocarpa* (*P. trichocarpa*) [13], showing that the *OSCA* gene family is ubiquitous in plants. Studies have shown that the *OSCA* gene family plays an important role in coping with adverse environmental conditions [7,11–13]. The overexpression of *ZmOSCA2.4* in *A. thaliana* significantly enhanced the drought resistance and reduced the expression of aging-related genes [14]. In tomato (*Solanum habrochaites*), all *SIOSCAs* respond to drought, and they respond to low temperature through the ABA signaling pathway [15]. *GmOSCA3.2,* expressed in soybean (*Glycine max* Merrill), showed an increased flower, leaf, and root growth under drought stress. Additionally, the *GmOSCA3.1* has also been up-regulated under alkali stress [16]. However, the *OSCA* gene family has not yet been identified and analyzed in *L. chinense.* (Hemsl.). Sarg., a member of the Magnoliaceae family of plants, is primarily distributed in the hilly regions of south China to the south of the Yangtze River. It is a significant species of premium timber and gardens attractive trees, yet the geographical distribution is affected by the climate factor, including the temperature and precipitation [17]. The completion of the whole genome sequencing of *L. chinense* provides an opportunity to analyze the *L. chinense* gene family [18]. To our knowledge, the function of *L. chinense* OSCAs has not been reported yet, thus rendering an incomplete understanding of the mechanism by which *L. chinense* responds to external stress signals. In this study, there were 11 members in the *OSCA* gene family of *L. chinense* which were unevenly distributed on eight chromosomes. We examined LchiOSCAs' physicochemical characteristics, transmembrane sections, phylogenetic relationships, conserved motifs, gene structure, cis-acting elements, and predicted their 3D structures. By using transcriptome (RNA-seq) analysis and qRT-PCR analysis, we also examined the *LchiOSCAs* expression patterns under abiotic stresses. Our findings will contribute to the functional analyses of LchiOSCAs and provide a knowledge base for future research.

2. Materials and Methods

2.1. Identification and Sequence Analysis of OSCA Genes in L. chinense

In order to study the evolutionary relationship of the *OSCA* gene family from lower plants to higher plants, 30 plant species protein sequences including: algae (*Chlamydomonas reinhardtii* and *Volvox carteri*), mosses (*Marchantia polymorpha* and *Physcomitrella patens*), ferns (*Selaginella moellendorffii*), Gymnosperms (*Cycas panzhihuaensis*), basal angiosperms (*Nymphaea colorata* and *Amborella trichopoda*), dicotyledons (*Arabidopsis thaliana*, *Capsella grandiflora*, *Capsella rubella*, *Daucus carota*, *Cucurbita moschata*, *Camellia sinensis*, *Vitis vinifera*, *Salix purpurea*, *Populus trichocarpa*, *Gossypium hirsutum* (*G. hirsutum*), *Glycine max*, *Theobroma cacao*, *Malus domestica* and *Eucalyptus grandis*), Magnolia (*Cinnamomum kanehirae*), and monocotyledons (*Spirodela polyrrhiza*, *Brachypodium distachyon*, *Oryza sativa*, *Zea mays* (*Z. mays*), *Sorghum bicolor*, *Panicum hallii* and *Setaria italica*) were download from the Phytozome (https://phytozome-next.jgi.doe.gov/, accessed on 10 September 2022) and NCBI website (https://www.ncbi.nlm.nih.gov/, accessed on 10 September 2022). The *L. chinense* protein sequences were downloaded from the genome database (https://hardwoodgenomics.org/Genome-assembly/2630420, accessed on

1 July 2022). The *OSCA* gene superfamily members of these plant species were identified by BLASTP using 15 *A. thaliana* OSCA protein sequences downloaded from the TAIR database (https://www.arabidopsis.org, accessed on 1 July 2022); with parameters: >30%, and E-value < 1×10^{-20} and/or E-value < 1×10^{-5}. The Hidden Markov Model of the DUF221 domain (PFAM accession number: 02714; http://pfam.xfam.org/, accessed on 1 July 2022) was used to verify the candidate OSCA members identified. In the *L. chinense* OSCA family and obtained at both parameters (>30%, and E-value < 1×10^{-20} and/or E-value < 1×10^{-5}) were further screened to remove the redundant sequences, and the *OSCA* gene domain was determined using the NCBI-CDD (https://www.ncbi.nlm.nih.gov/Structure/cdd/wrpsb.cgi, accessed on 1 July 2022), SMART (http://smart.embl-heidelberg.de/, accessed on 1 July 2022), and Pfam databases [19,20].

To analyze the sequence characteristics of the protein, such as the amino acid length (AA length), molecular weight (MW), and the theoretical isoelectric point (PI), we used the ExPASY tool (https://web.expasy.org, accessed on 1 July 2022). The subcellular localization of plant proteins was predicted using WoLFPSORT (https://wolfpsort.hgc.jp/, accessed on 1 July 2022) and Plant-mPLoc (http://www.csbio.sjtu.edu.cn/bioinf/plant-multi/, accessed on 1 July 2022). The identified LchiOSCA genes were renamed according to their chromosomal positions.

2.2. Phylogenetic Analysis and Sequence Alignment

To explore the evolutionary relationship of all 31 species, we used the OrthoFinder software (v2.5.4) using full length protein sequences, and the MSA gene tree inference and DIAMOND software (v0.9.25) were used for a quick BLAST. Multiple sequence alignments were constructed using the MAFFT, and the IQ-TREE was utilized to construct the maximum likelihood species tree inference [21]. To gain an insight into the evolutionary relationship of the *OSCA* gene superfamily, the *Arabidopsis* AtOSCAs (*A. thaliana*), rice OsOSCAs (*O. sativa*), and *Populus* PtOSCAs (*P. trichocarpa*) information was extracted from previous publications [7,11,13]. Jalview software (https://www.jalview.org/, accessed on 15 July 2022) was utilized for the protein multiple sequence alignments while the MEGA-X software with a bootstrap value set at 1000 [22], was used to construct the phylogenetic evolutionary tree (neighbor-joining). Additionally, the EvolView online tool was used to beautify the phylogenetic tree (https://evolgenius.info/, accessed on 15 July 2022) [23]. The TMHMM server v2.0 website (http://www.cbs.dtu.dk/services/TMHMM/, accessed on 15 July 2022) was used to predict the transmembrane regions in the conserved regions of the DUF221 [24].

2.3. Gene Structure and Protein Conserved Motif Analysis

The gene structure and conserved motif arrangement knowledge provides a base for the biochemical function prediction, to have an insight into the gene structure and conserved motif arrangements. The MEME tool (http://meme-suite.org/tools/meme, accessed on 15 July 2022) was used, with a parameter set at 10 (total number of motifs) and other as the default. The gene structure of the *LchiOSCA* genes were generated by the Tbtools using the GFF3 files and protein sequences of the *L. chinense* genome [25,26].

2.4. Chromosomal Location and Collinearity Analysis of LchiOSCA Genes

Information on the chromosomal location of the *OSCA* genes was obtained according to the genome annotation file of the *L. chinense* genomic data and annotation. The files of *A. thaliana*, *O. sativa,* and *P. trichocarpa* were downloaded from the Ensembl plant's database (http://plants.ensembl.org/index.html, accessed on 1 July 2022). Tandem duplication refers to the localization of two or more members of a family within the same chromosome and in neighboring intergenic regions [27]. Gene pairs between *L. chinense* and *A. thaliana*, *O. sativa*, and *P. trichocarpa* were aligned and analyzed using the MCScanX function in Tbtools. The collinearity and chromosomal localization were plotted using the circos function in the Tbtools software. The synonymous substitution rate (Ks) and nonsynonymous

substitution rate (Ka) were calculated for gene pairs using the "Simple Ka/Ks calculator" tool in TBtools [26].

2.5. Analysis of Cis-Acting Elements in the Promoter of LchiOSCA Genes

The sequences of 2000 bp upstream of the coding sequence (CDS) of the *OSCA* genes were extracted from the *L. chinense* genome, and the obtained data were uploaded on the PlantCARE website (http://bioinformatics.psb.ugent.be/webtools/plantcare/html/, accessed on 15 July 2022). The Tbtools software was used to graphically present the hormone and abiotic stress-related cis-acting elements in the promoter [25].

2.6. Three-Dimensional (3D) Structure Prediction of LchiOSCAs

The protein structure governs the specific function of a protein in any organism, and many protein functions rely on a proper folding and conformation. Homology modeling based on the analytical structure of the homologous proteins can be used to predict the 3D structural modeling of the LchiOSCA proteins. First, we used the SWISS-MODEL website (https://swissmodel.expasy.org, accessed on 15 July 2022) to predict the 3D structure of LchiOSCAs, and then we visualized it using the Chimera software (v1.16) (http://www.cgl.ucsf.edu/chimera/index.html, accessed on 15 July 2022) [28].

2.7. Expression Analysis of LchiOSCA Genes

The seedlings of *L. Chinense* were grown in a greenhouse for two weeks (16 h of daylight followed by 8 h of darkness, 22–25 °C, and 70% relative humidity). To simulate cold, heat, or drought stress, the plants were placed at 4 °C or 40 °C or 15% PEG6000 for 1 h, 3 h, 6 h, 12 h, 1 day, and 3 days, respectively, referred to in the previous reports by Li et al. [29]. A homologous comparison and qRT-PCR primer design for the selected sequences were conducted using the Jalview software (v2.11.2.5) and the Primer3plus online website (https://www.primer3plus.com, accessed on 15 July 2022). Using 18 s rRNA as the internal reference (Supplementary Table S1), the significance analysis (* $p < 0.05$, ** $p < 0.01$) was performed using Student's *t*-test in SPSS software (v26.0), and graphs of the data were constructed using GraphPad Prism (v9.0.0).

3. Results

3.1. Identification of OSCA Genes in 31 Plant Species

After eliminating the redundant and incomplete sequences, 399 OSCA proteins were identified in 31 plant species (Figure 1 and Table S2). Out of all of the species investigated, *G. hirsutum* had the greatest number of *OSCA* genes (37), a number nine-fold greater than that which was observed in *M. polymorpha* (4). The remaining 29 plant species contained 5 to 22 *OSCA* genes. We found many OSCA candidates in angiosperms and relatively few *OSCA* candidates in lower plants. Among the higher plants, *G. hirsutum* as an allotetraploid had the highest number of proteins, while other higher plant species had 8–22 proteins.

In addition, we used OrthoFinder (v2.5.4) to explore the OSCA evolution status of all 31 plants, and phylogenetic analysis showed that the OSCA evolution status of *L. chinense* was closer to that of *C. kanehirae*. The evolutionary status of both plants is higher than that of algae, mosses, ferns, gymnosperms, and basal angiosperms, but it is lower than the higher angiosperms (Figure 1).

3.2. Sequence Characterization of OSCA Family Members of L. chinense

The identified 11 *L. chinense OSCA* genes were renamed as LchiOSCA1 to LchiOSCA11 (Table 1), based on their choromosomal localizations. The LchiOSCAs were unevenly located on 8 of the 19 chromosomes. The physiochemical property analysis showed that the amino acid length of the OSCA proteins in *L. chinense* ranged from 389 (LchiOSCA5) to 769 (LchiOSCA3), with an average of 599. The molecular weight (MW) ranged from 43.79 (LchiOSCA5) to 88.24 kDa (LchiOSCA3) and the isoelectric points (pI) values ranged from 8.62 (LchiOSCA6) to 9.54 (LchiOSCA1). The protein hydrophilicity analysis showed that all

the LchiOSCAs were hydrophobic proteins with a hydrophilicity index greater than 0. The subcellular localization analysis showed that all LchiOSCAs were located on the plasma membrane (Table 1).

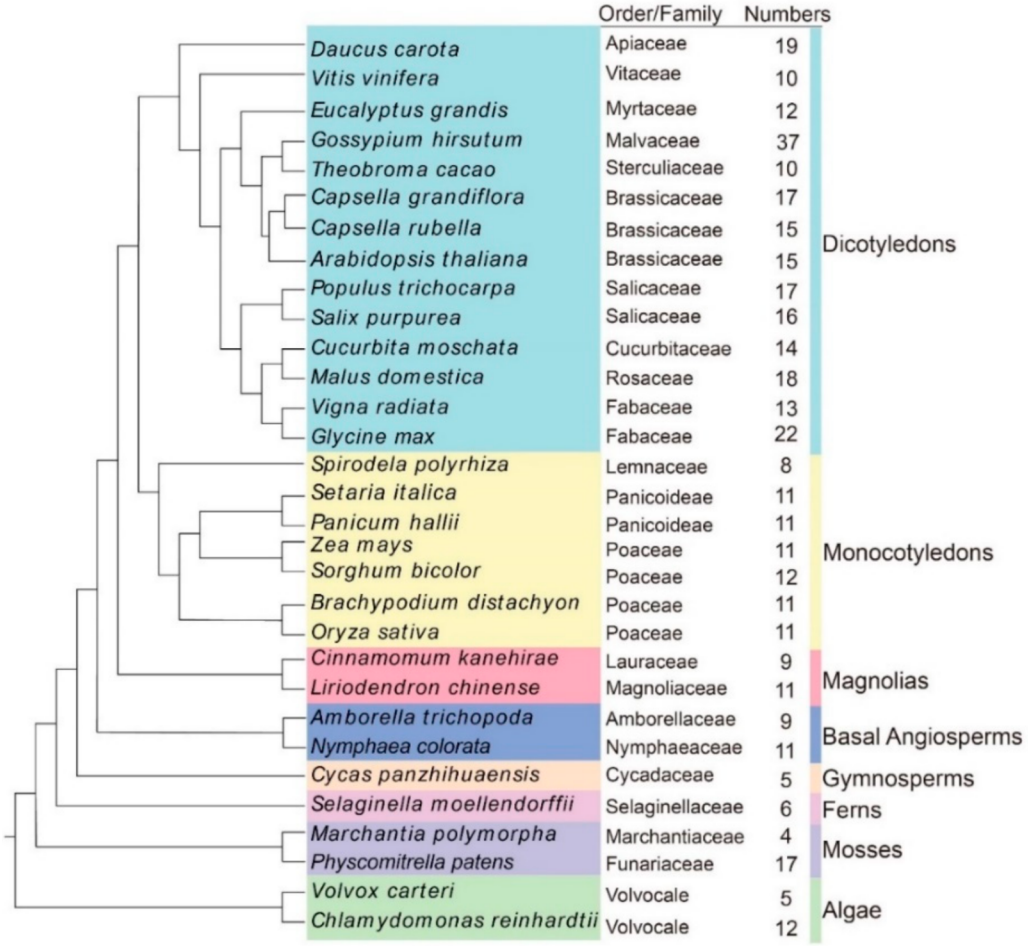


Figure 1. Phylogenetic relationships of the 31 species *OSCA* genes. OrthoFinder (v2.5.4) was used to construct the phylogenetic tree of 31 species of OSCA protein. Different colors from top to bottom represent gymnosperm, fern, mosses, basal angiosperms, magnolias, dicotyledons, and monocotyledons, respectively. To the left side of each evolutionary branch of species is the name of the family.

Table 1. Characteristics information of *OSCA* genes in *L. chinense*.

Gene Name	Gene ID	Chr	AA Length	PI	MW (KDa)	Predicted Localization	GRAVY
LchiOSCA1	Lchi30427	1	708	9.54	80.36	Plasma membrane	0.258
LchiOSCA2	Lchi30428	1	670	9.45	75.52	Plasma membrane	0.24
LchiOSCA3	Lchi26953	3	769	9.42	88.24	Plasma membrane	0.124
LchiOSCA4	Lchi26954	3	768	9.03	87.59	Plasma membrane	0.173
LchiOSCA5	Lchi11206	4	389	9.16	43.79	Plasma membrane	0.203
LchiOSCA6	Lchi32997	7	402	8.62	45.74	Plasma membrane	0.405
LchiOSCA7	Lchi27474	7	619	9.15	70.37	Plasma membrane	0.298
LchiOSCA8	Lchi08358	8	684	9.48	78.60	Plasma membrane	0.156
LchiOSCA9	Lchi00390	9	757	8.81	86.04	Plasma membrane	0.342
LchiOSCA10	Lchi10862	13	418	9.33	46.20	Plasma membrane	0.322
LchiOSCA11	Lchi11122	19	402	9.45	45.97	Plasma membrane	0.698

3.3. Conserved Domain and Transmembrane Domain Analysis of LchiOSCAs

The TMHMM online program was used to estimate the transmembrane domains of the *L. chinense* OSCA proteins. We found that each *L. chinense* OSCA had a large number of transmembrane domains (5–10). The transmembrane domains were mostly distributed at both ends of the protein, with 2–3 at the N-terminus and 6–7 at the C-terminus. The LchiOSCAs proteins contained more than eight transmembrane domains, except LchiOSCA5, −6, −8, and −10 (Figure 2 and Figure S1), suggesting a deletion event in these four proteins. Taken together, the presence of transmembrane domains also implies that these proteins should be localized in the membrane system.

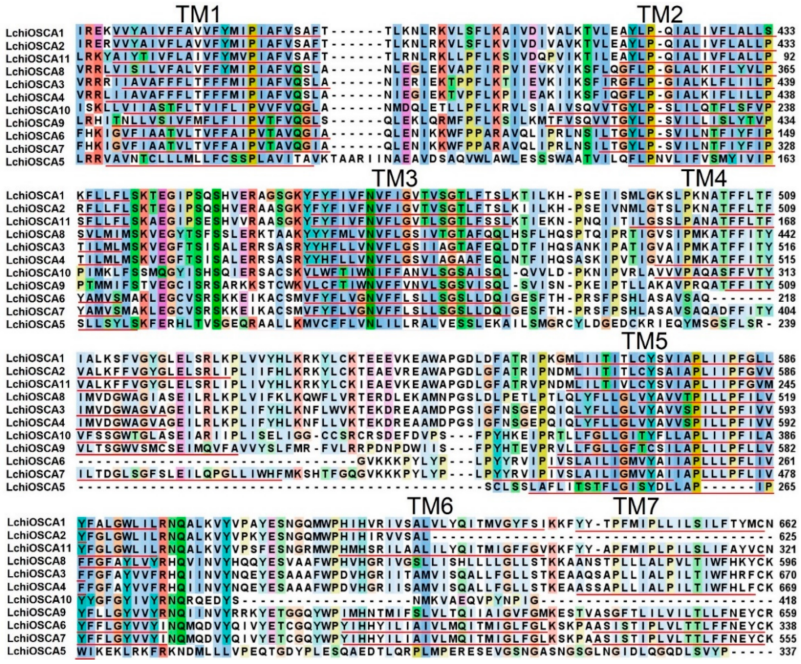


Figure 2. DUF221 functional domain protein sequence alignment and transmembrane domain prediction of LchiOSCAs. Transmembrane domains TM1–TM7 were annotated by red underlines.

3.4. Phylogenetic Analysis and Classification of L. chinense *OSCA Gene Family*

To understand the functional characteristics and evolutionary relationship of the *OSCA* gene family in *L. chinense*, a phylogenetic tree was constructed using the full-length sequences of the OSCA proteins in *L. chinense* (11), *A. thaliana* (15), *O. sativa* (11), and *P. trichocarpa* (17). Based on the phylogenetic tree, the OSCA proteins can be divided into four subgroups (Clade 1–4) (Figure 3). The results showed that the LchiOSCAs were unevenly distributed in the four subfamilies, among which the Clade 2 subfamily had the largest number of the LchiOSCA proteins, and Clade 4 had only one member (LchiOSCA5) (Supplementary Table S3), suggesting that this gene has been preserved in the process of evolution and is conserved in dissimilar species, and that it plays vital roles in plants.

3.5. Analysis of OSCA Gene Structure and Conserved Domain in L. chinense

Understanding the gene evolution provides a base for understanding the gene structure and the conserved motifs. The gene structure investigations showed that the *LchiOSCA* gene family members in the same phylogenetic group had similar gene arrangements. The *LchiOSCA* gene intron counts ranged from 1 to 11 (Figure 4C). Specifically, the Clade 1 subfamily members had an average number of 10 introns, the Clade 2 subfamily members had 9, the Clade 3 subfamily members had 5, and the Clade 4 subfamily members had only 1 intron. We speculated that the *LchiOSCA5* had only one intron due to the short length of the gene, and consequently we concluded that *LchiOSCA5* may have lost some functions in the process of evolution (Figure 4A,C).

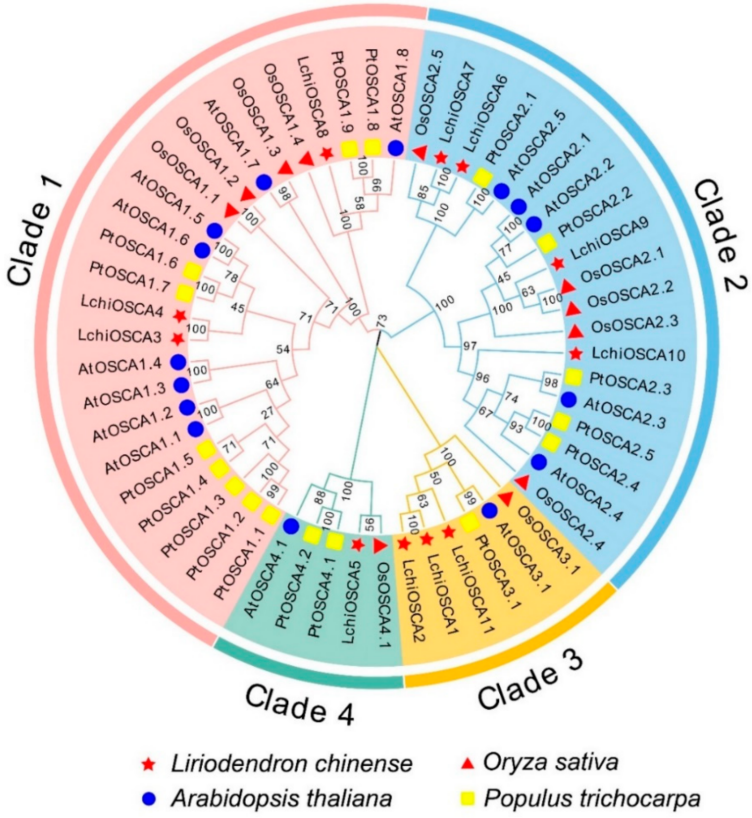


Figure 3. Phylogenetic tree analysis of *OSCA* gene family in *L. chinense*, *A. thaliana*, *O. sativa*, and *P. trichocarpa*. The Clade 1 to 4 are shaded by Jade red, with blue, orange, and aquatic green, respectively. Genes from *L. chinense* (Lchi), *A. thaliana* (At), *O. sativa* (Os), and *P. trichocarpa* (Pt) are marked by a red star, blue circle, red triangle, and yellow rectangle in the inner circle, respectively.

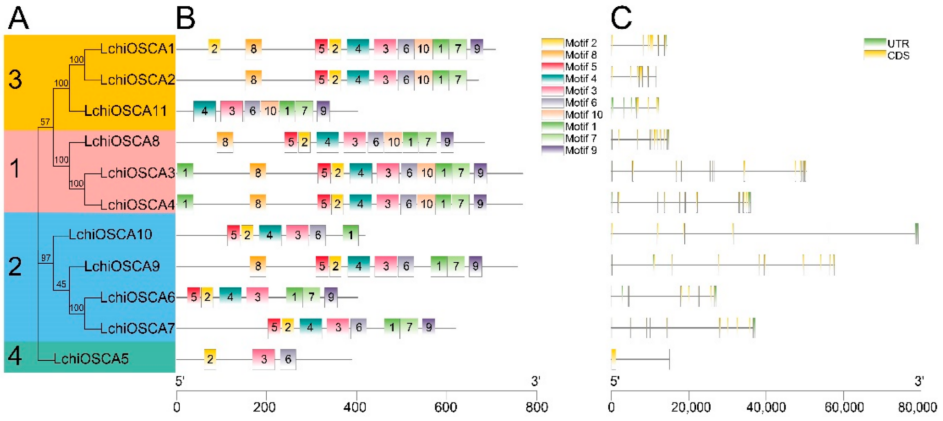


Figure 4. The gene structure and conserved motifs of *LchiOSCA* genes. (**A**) The phylogenetic tree was constructed with OSCA proteins from *L. chinense*. The sequence information for each motif was provided in Supplementary Table S4. (**B**) Conserved motifs arrangement of LchiOSCAs. (**C**) Exon-intron patterns.

The MEME software predicted 10 motifs in the *L. chinense OSCA* genes (Figures 4B and S2). Motif 3 was present in all the LchiOSCA proteins, indicating that the Motif 3 is relatively highly conserved. Motif 9 was absent in LchiOSCA2, LchiOSCA5, and LchiOSCA10 (Supplementary Table S4). We also noted that the *L. chinense OSCA* genes grouped together had a similar Motif number and arrangements. For instance, Clade 1 had a similar Motif number and arrangement. Thus, we concluded that the *L. chinense*

OSCA genes may have similar functions. In general, we showed that the higher the gene homology, the stronger the motif similarity arrangement.

3.6. Gene Duplication and Divergence of LchiOSCA Genes

According to the location information of the *OSCA* genes in *L. chinense*, we found that 11 genes were unevenly distributed on eight chromosomes. There are two members distributed on chromosomes 1, 3, and 7, and only one member was present on the remaining five chromosomes. As shown in Figure 5, two tandem duplication events were detected between the 11 *OSCA* genes, accounting for 36% (4/11) of the *OSCA* gene families. Gene pairs included *LchiOSCA1/LchiOSCA2* (which belonged to Clade 3) and *LchiOSCA3/LchiOSCA4* (which belonged to Clade 1). However, we did not detect segmental duplications of the *LchiOSCA* genes.

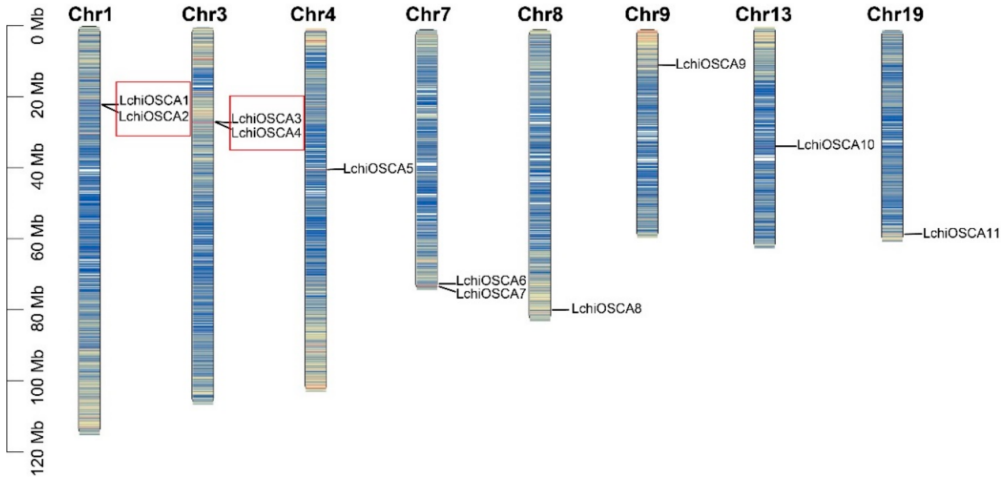


Figure 5. Distribution of *OSCA* family genes on chromosomes in *L. chinense*. The tandem duplicated gene pairs were marked by red boxes. Different colors represent gene density on the chromosome and blue to red represent low density to high density.

To gain a further insight into whether the *LchiOSCA* family genes have been subject to natural selection pressure during evolution and to trace their time of replication, the Ka, Ks, and Ka/Ks ratios were calculated for the duplicated genes in *L. chinense* (Supplementary Table S5). The Ka/Ks ratios for the two *LchiOSCA* tandem duplication gene pairs were 0.347 and 0.333, with an average of 0.34.

3.7. Synteny Analysis of LchiOSCA Genes among L. chinense, A. thaliana, O. sativa and P. trichocarpa

To gain a further insight into the phylogenetic mechanism of the *LchiOSCA* gene family, comparative synteny maps were conducted among two dicots (*A. thaliana* and *P. trichocarpa*) and one monocot (*O. sativa*) (Figure 6). The results revealed that *L. chinense* and *P. trichocarpa* had five pairs of collinear genes, and two pairs of collinear members were present in both *A. thaliana* and *O. sativa*. The results presented that most *L. chinense OSCA* homologs were present in *P. trichocarpa*, followed by *A. thaliana* and *O. sativa*. The analysis of the evolutionary selective pressures on these collinear members revealed Ka/Ks ratios of less than one (Supplementary Table S6), indicating that they have all been subjected to a purifying selection during evolution. Furthermore, we found that *LchiOSCA8* and *LchiOSCA11* had collinear gene pairs in three species: *A. thaliana*, *O. sativa*, and *P. trichocarpa*, and the results showed that these two genes remained stable in different species throughout their long evolution.

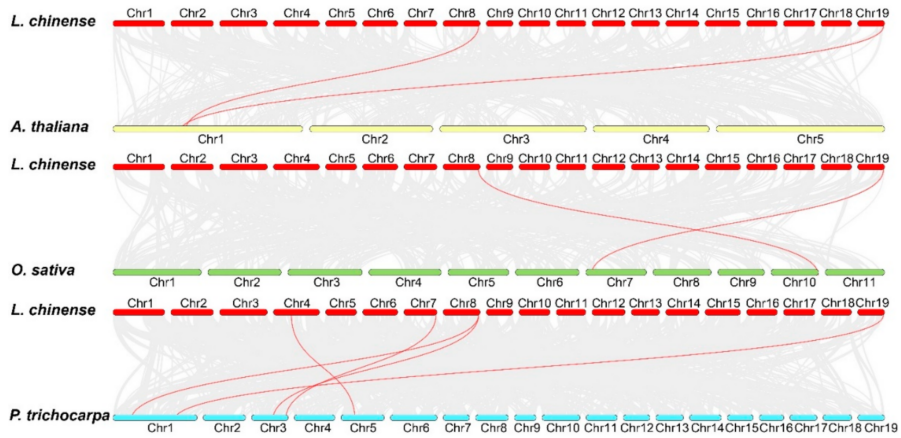


Figure 6. Collinearity analysis of *OSCA* family members in *L. chinense* and *A. thaliana*, *L. chinense* and *O. sativa*, and *L. chinense* and *P. trichocarpa*. Gray lines in the background indicate the collinear blocks within the *L. chinense* and other plant genomes, and the syntenic *OSCA* gene pairs were highlighted with red lines.

3.8. Analysis of Cis-Acting Elements in the Promoter Region of OSCA Genes in L. chinense

Cis-acting elements in the promoter regions play significant roles in regulating the gene expression. The cis-acting elements related to the plant hormone response and abiotic stress were analyzed in the *LchiOSCAs* promoter region and predicted 136 cis-acting elements (Supplementary Table S7). Among them, *LchiOSCA5* had the most cis-acting elements related to the hormone regulation and stress factors (19), and *LchiOSCA6* had the least amount of cis-acting elements (5) (Figure 7C). According to the statistical results, the ABRE elements were more prevalent, and not present in *LchiOSCA10*. *LchiOSCA7*, *LchiOSCA8*, and *LchiOSCA5* had more MeJA response elements, and the LTR were specifically distributed in *LchiOSCA1*, *−3*, *−4*, *−5*, and *−7*. In addition, we found that the cis-acting elements of different gene promoters were very different. Even in the same subfamily, there were obvious differences, especially in the salicylic acid response elements and low temperature response elements. For instance, only one member of the second subfamily of *LchiOSCAs* had low temperature response elements, while two members lack the salicylic acid response elements. The drought response elements and abscisic acid response elements were found only in *LchiOSCA1*, *−2*, *−9*, and *−11*, suggesting that these conditions may be intimately connected (Figure 7B,C and Supplementary Table S7).

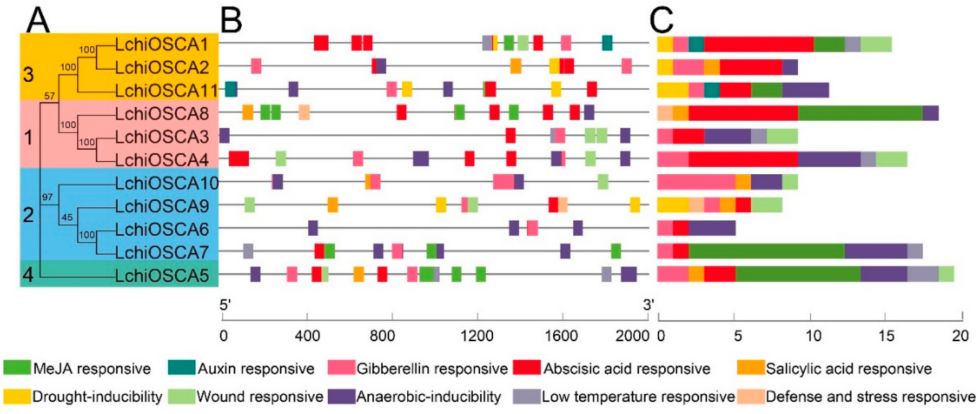


Figure 7. Cis-acting elements of abiotic stress and hormone response in the *LchiOSCAs* promoter region. (**A**) The phylogenetic tree was constructed with OSCA proteins from *L. chinense*. (**B**) Locations of cis-acting elements in the 2 kb sequences upstream of *LchiOSCAs*, different colored squares represent different types of cis-acting elements. (**C**) The sum of the cis-acting elements in each *LchiOSCA* is represented by a histogram of different colors.

3.9. Prediction of the Three-Dimensional (3D) Structures of LchiOSCAs

To have a deeper understanding of the possible mechanism of action of the OSCA proteins in *L. chinense*, we performed a homology modeling of all the OSCA proteins (Figure 8). The results showed that the GMQE scores of all the models ranged from 0.48 to 0.7, with a high confidence (Supplementary Table S8). The same PDB hit indicated that their 3D structures were similar. LchiOSCA1–2, −5, and −11 (5z1f.1.A, CSC1-like protein ERD4) and LchiOSCA3–4, and 6–10 (6ijz.1.A, calcium-permeable stress-gated cation channel 1) presented the same PDB, indicating that there were some similarities in their 3D structures. The 3D structural models of these proteins provide a foundation to understand their biological functions.

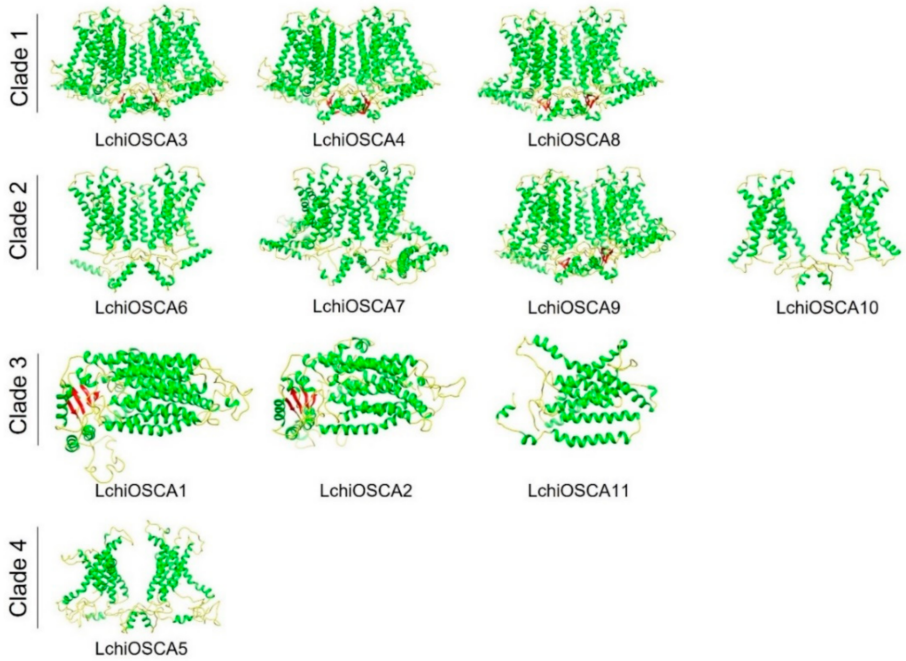


Figure 8. The 3D structure modeling of LchiOSCA proteins. The structured image was generated using the Chimera software (v1.16). The random coil, α-helix, and β-strand are marked by yellow, green, and red, respectively.

3.10. Differently Responsive Patterns of LchiOSCAs to Abiotic Stress

In order to understand the abiotic stress response characteristics of the *LchiOSCA* gene family, the expression pattern of the *LchiOSCA* genes was analyzed at seven time points (1 h, 3 h, 6 h, 12 h, 1 day, and 3 days) under drought, cold, and heat stress treatments. The TPM values of the genes under the three abiotic stresses are shown in Supplementary Table S9.

As shown in Figure 9A, the expression levels of the *LchiOSCA2*, *LchiOSCA4*, and *LchiOSCA8* genes were significantly induced after the drought stress. The expression levels of the *LchiOSCA2* and *LchiOSCA4* genes reached the highest expression after 1 day of drought stress. In addition, the *LchiOSCA2* and *LchiOSCA4* were highly expressed during all time points. These results may indicate that *LchiOSCA2* and *LchiOSCA4* mainly promote the response of *L. chinense* to the drought stress. Under cold stress, the gene expression of *LchiOSCA2*, *LchiOSCA4*, and *LchiOSCA9* were significantly increased, among which the expression of *LchiOSCA2* was the highest, followed by *LchiOSCA4*. Most of the genes were expressed at the highest levels at the 1 day and 3 days time points, indicating that 1 day and 3 days might be important response time points under the cold stress treatment conditions. *LchiOSCA1*, *−2*, *−3*, *−4*, and *−6* were highly expressed to various degrees under heat stress conditions. *LchiOSCA2*, *−4*, and *−9* showed the highest expression at 3 days, and *LchiOSCA6*, *−7*, and *−11* showed a low expression at almost all time points,

and we concluded that *LchiOSCA1*, *−2*, *−3*, *−4*, and *−9* may be the main responsive genes to high temperature stress (Figure 9B,C).

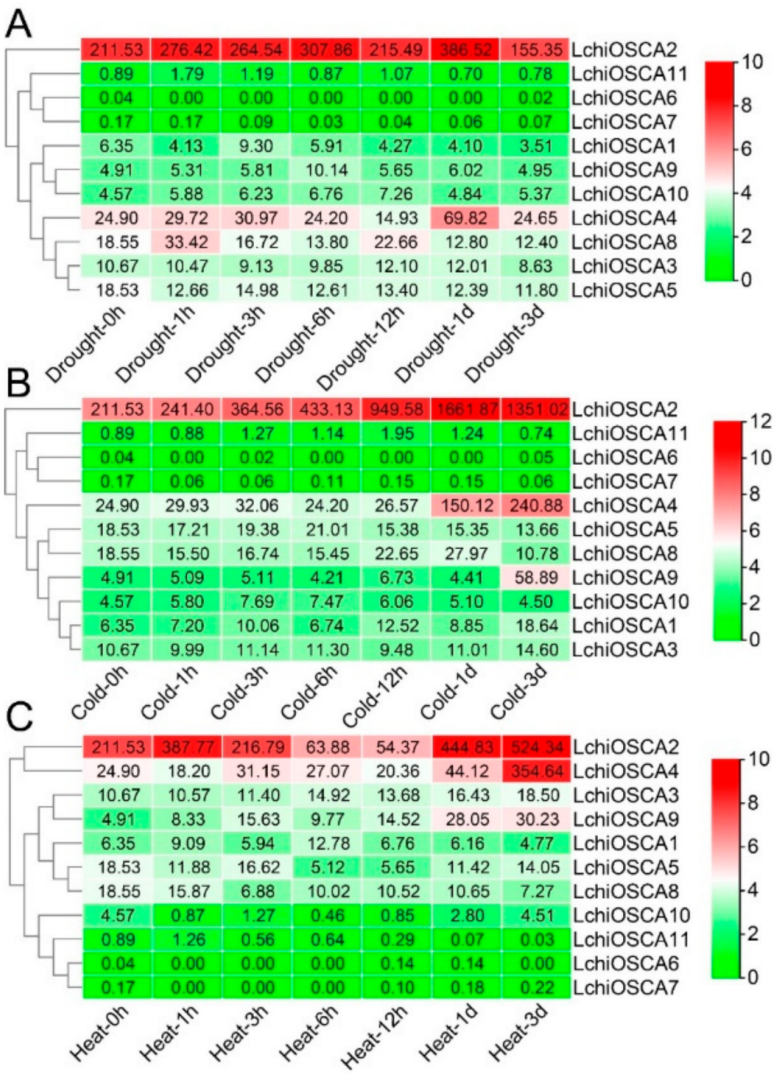


Figure 9. The expression patterns of *OSCA* gene family in drought stress (**A**), cold stress (**B**), and heat stress (**C**) of *L. chinense*. The expression levels of the genes were expressed by TPM. The hierarchical clustering of genes based on expression is shown on the left. The color scale picture on the far right, represents the log2 expression value, where green represents the low level and red represents the high level of transcript abundance. Gene names were enlisted on the right.

In order to verify the reliability of the transcriptome sequencing results, we used qRT-PCR to detect the gene expression of *LchiOSCA* genes under drought, cold, and heat stress treatments. The results showed that most of the *LchiOSCA* genes were up-regulated at different time points and at different levels under the drought treatment, but *LchiOSCA2* and *LchiOSCA4* particularly were significantly up-regulated at 6 h (Supplementary Figure S3). In the cold treatment, the expression of *LchiOSCA2* increased gradually until its peak expression at 6 h. In addition, *LchiOSCA4* and *LchiOSCA9* reached their highest levels at 3 days of cold stress treatment. Under heat stress, *LchiOSCA3-4* and *9* showed an expression peak point at 3 days, respectively.

Taken together, both *LchiOSCA2* and *LchiOSCA4* showed high expression levels under a low temperature, high temperature, and drought stress, and they were speculated to play a major role in the regulation of *L. chinense* stress responses.

4. Discussion

Plants have evolved complex signal transductions and stress resistance mechanisms to survive the harsh weather conditions of the external environmental [2,4]. The *OSCA* genes induce the increase in the Ca^{2+} concentration in the cytoplasm during hyperosmotic stress, which is an essential response mechanism of plants to drought and salt-induced osmotic stress [7,12,15]. The *OSCA* gene family members in plants that carry the DUF221 domain have been identified in plants such as: *A. thaliana* [7], *O. sativa* [11], *Z. mays* [30], *V. radiata* [12], and *P. trichocarpa* [13]. This experiment identified a total of 11 *LchiOSCA* gene family members, all containing a DUF221 domain and showing some response to adversity stress, based on the whole genome sequencing data of *L. chinense*. Multiple transmembrane domains have been found in LchiOSCA proteins carrying the DUF221 domain that contains 6–7 transmembrane domains, as previously reported (Figure 2, Table 1) [11,30]. Compared with most of the monocotyledons, the *LchiOSCA* gene number is less. This may be related to its evolutionary status and the fact that the *L. chinense* is relatively close to the basal angiosperms, as compared to the higher angiosperms (Figure 1).

The phylogenetic analysis indicated that the LchiOSCA family can be divided into four groups, which is consistent with previous studies on *A. thaliana*, *O. sativa*, *Z. mays*, *G. hirsutum*, and *P. trichocarpa*, and also indicates that the conservation of these sequences is consistent to other studies (Figure 3) [7,11,12,30,31]. A further analysis exhibited that the species closest to the OSCA family of *L. chinense* was *P. trichocarpa*, followed by *O. sativa*, and *A. thaliana* was the furthest. Gene replication is an important mechanism of genome evolution, a prerequisite for the diversity of gene functions, and the main reason for the expansion of gene families. A further analysis revealed that each group included the members of the OSCA family from monocot *O. sativa* and dicot *A. thaliana*, *L. chinense,* and *P. trichocarpa*, indicating that the OSCA family was genetically diverse before the divergence of monocots and dicots. Members of Clade 3 and 4 in the OSCA family are rare, but both have been retained during evolution, suggesting that they may have played important roles in plant evolution. At the same time, interspecies collinearity showed that more *OSCA* gene pairs existed in *L. chinense* and *P. trichocarpa*, possibly resulting from trees in both species with close affinities (Figure 6).

The cis-acting element analysis identified multiple hormone-responsive elements and stress (low temperature, drought) responsive elements present in most of the *LchiOSCAs* promoter regions (Figure 7). This result suggests that *LchiOSCAs* can respond to external environmental stress. Related studies have considered that the ABA signaling pathway is a central regulator of abiotic stress responses in plants, triggering gene expression and adaptive physiological response changes [32–34]. According to the research by Colebrook et al., an exogenous gibberellin (GA3) administration might stimulate the production of salicylic acid (SA), which would then counteract the negative effects of abiotic stress on the seedling stage of plants [35]. Additionally, some research contends that jasmonic acid (JA) interacts both synergistically and antagonistically with other phytohormones such as abscisic acid (ABA), ethylene (ET), and salicylic acid (SA), and others act independently in regulating plant tolerance to environmental stress [36]. Therefore, we hypothesize that the *OSCA* gene family members can trigger a chain reaction to combat the negative impacts brought on by the environment by spraying various exogenous hormones, so ensuring plants develop normally.

The *OSCA* genes play important roles in plant abiotic stress regulation. The overexpression of maize *ZmOSCA2.4* in *A. thaliana* significantly improves the drought resistance [14]. The overexpression of *OsOSCA1.1* or *OsOSCA2.2* enhanced the *A. thaliana* tolerance to a high osmolality and salt stress treatments [37,38]. Researchers found that *OsOSCA2.1*, *−2.5*, and *−3.1* were significantly upregulated under salt stress and PEG stress [11]. In mung bean, the expression of *VrOSCA1.4*, *−2.2*, *−2.4*, *−2.5*, *−2.6*, and *−3.1* genes were also significantly induced after the PEG treatment [12]. This study analyzed the responses of *OSCA* genes in *L. chinense* under drought, low temperature, and high temperature stress conditions. Some *LchiOSCAs* were expressed under three stress conditions, while others

were expressed under only one or two stress conditions. For example, *LchiOSCA2* and *LchiOSCA4* respond strongly to drought, low temperature, and high temperature stress, indicating that there is an interaction in the response pathway of *LchiOSCA2* and *LchiOSCA4* to the three stress conditions. *LchiOSCA9* was highly expressed under drought and heat stress and lowly expressed under cold stress. *LchiOSCA8* was significantly induced only under drought stress. Therefore, we concluded that the *LchiOSCA2* may be the primary regulating gene during abiotic stress, due to its high expression under three separate abiotic stresses at different times. (Figure 9). The findings of this work may offer fundamental theoretical support for understanding the roles played by *L. chinense OSCA* family members and the molecular processes underlying their reactions to stress and adversity. In turn, it will provide gene resources for genetic improvement by gene editing and transformation.

5. Conclusions

In this study, OSCA members from 31 species were identified ranging from lower plants to higher plants, with a total of 399 proteins. A total of 11 LchiOSCA family members were identified and divided into four subgroups, which were distributed on eight chromosomes. The analysis of the gene structures, conservative motifs, and 3D protein structures further proved the results of the phylogenetic tree. The gene replication events and Ka/Ks analysis showed that the *LchiOSCA* family expanded mainly through the tandem replication events and was affected by a purification selection during evolution. In addition, *LchiOSCAs* participates in the response to various abiotic stresses, *LchiOSCA2* and *LchiOSCA4* cross regulate the response to drought, cold, and heat stress. The above results provide a reference for further research on the biological function of the *OSCA* gene family of *L. chinense* and its regulation mechanism in response to abiotic stress.

Supplementary Materials: The following supporting information can be downloaded at: https://www.mdpi.com/article/10.3390/f13111835/s1, Figure S1: Putative transmembrane domains of LchiOSCAs; Figure S2: Specific information of each motif; Figure S3: Expression analysis of *LchiOSCA* genes in response to drought, cold and heat stress. Expression analysis of *LchiOSCA* genes by qRT-PCR. 0 h, 6 h and 3 d represent the treatment times of various stresses; Table S1: The primers used in the qRT-PCR; Table S2: The IDs of plant OSCA proteins; Table S3: Information of *OSCA* genes from *L. chinense, A. thaliana, O. sativa, and P. trichocarpa*; Table S4: Details of motifs in LchiOSCA proteins identified by MEME; Table S5: The Ka/Ks ratios for duplicated *LchiOSCA* genes; Table S6: Analysis of evolutionary selection pressure on collinear members of *OSCA* family in *L. chinense* and *A. thaliana*, *L. chinense* and *O. sativa*, and *L. chinense* and *P. trichocarpa*; Table S7: Predicted cis-elements results; Table S8: Structural dependent modeling parameters for the OSCA proteins; Table S9: TPM value of drought, cold and heat stress.

Author Contributions: Y.K., L.Y. and J.C. conceived and designed this research; M.X., R.L. and Y.G. performed the experiments; D.H. and B.A. assisted with the analysis and interpretation of the data. All authors have read and agreed to the published version of the manuscript.

Funding: This research was funded by the National Natural Science Foundation of China (No. 31971682, 32071784), Youth Foundation of the Natural Science Foundation of Jiangsu Province (No. BK20210614), The Priority Academic Program Development of Jiangsu Higher Education Institutions (PAPD), and the Research Startup Fund for High-Level and High-Educated Talents of Nanjing Forestry University.

Data Availability Statement: Not applicable.

Conflicts of Interest: The authors declare no conflict of interest. The funders had no role in the design of the study; in the collection, analyses, or interpretation of data; in the writing of the manuscript; or in the decision to publish the results.

References

1. Zhang, H.; Zhu, J.; Gong, Z.; Zhu, J. Abiotic stress responses in plants. *Nat. Rev. Genet.* **2022**, *23*, 104–119. [CrossRef] [PubMed]
2. Peck, S.; Mittler, R. Plant signaling in biotic and abiotic stress. *J. Exp. Bot.* **2020**, *71*, 1649–1651. [CrossRef] [PubMed]

3. Gong, Z. Plant abiotic stress: New insights into the factors that activate and modulate plant responses. *J. Integr. Plant Biol.* **2021**, *63*, 429–430. [CrossRef] [PubMed]
4. Zhang, Y.; Lv, Y.; Jahan, N.; Chen, G.; Ren, D.; Guo, L. Sensing of abiotic stress and ionic stress responses in plants. *Int. J. Mol. Sci.* **2018**, *19*, 3298. [CrossRef]
5. Dodd, A.N.; Kudla, J.; Sanders, D. The language of calcium signaling. *Annu. Rev. Plant Biol.* **2010**, *61*, 593–620. [CrossRef]
6. Koster, P.; DeFalco, T.; Zipfel, C. Ca^{2+} signals in plant immunity. *EMBO J.* **2022**, *41*, e110741. [CrossRef]
7. Yuan, F.; Yang, H.; Xue, Y.; Kong, D.; Ye, R.; Li, C.; Zhang, J.; Theprungsirikul, L.; Shrift, T.; Krichilsky, B.; et al. OSCA1 mediates osmotic-stress-evoked Ca^{2+} increases vital for osmosensing in *Arabidopsis*. *Nature* **2014**, *514*, 367–371. [CrossRef]
8. Jojoa-Cruz, S.; Saotome, K.; Murthy, S.E.; Tsui, C.C.A.; Sansom, M.S.; Patapoutian, A.; Ward, A.B. Cryo-EM structure of the mechanically activated ion channel OSCA1.2. *Elife* **2018**, *7*, e41845. [CrossRef]
9. Liu, X.; Wang, J.; Sun, L. Structure of the hyperosmolality-gated calcium-permeable channel OSCA1.2. *Nat. Commun.* **2018**, *9*, 5060. [CrossRef]
10. Zhang, M.; Wang, D.; Kang, Y.; Wu, J.X.; Yao, F.; Pan, C.; Yan, Z.; Song, C.; Chen, L. Structure of the mechanosensitive OSCA channels. *Nat. Struct. Mol. Biol.* **2018**, *25*, 850–858. [CrossRef]
11. Li, Y.; Yuan, F.; Wen, Z.; Li, Y.; Wang, F.; Zhu, T.; Zhuo, W.; Jin, X.; Wang, Y.; Zhao, H.; et al. Genome-wide survey and expression analysis of the OSCA gene family in rice. *BMC Plant Biol.* **2015**, *15*, 261. [CrossRef]
12. Yin, L.; Zhang, M.; Wu, R.; Chen, X.; Liu, F.; Xing, B. Genome-wide analysis of OSCA gene family members in *Vigna radiata* and their involvement in the osmotic response. *BMC Plant Biol.* **2021**, *21*, 408. [CrossRef] [PubMed]
13. Hartmann, F.P.; Tinturier, E.; Julien, J.L.; Leblanc-Fournier, N. Between stress and response: Function and localization of mechanosensitive $Ca^{(2+)}$ channels in herbaceous and perennial plants. *Int. J. Mol. Sci.* **2021**, *22*, 11043. [CrossRef] [PubMed]
14. Cao, L.; Zhang, P.; Lu, X.; Wang, G.; Wang, Z.; Zhang, Q.; Zhang, X.; Wei, X.; Mei, F.; Wei, L.; et al. Systematic analysis of the maize OSCA genes revealing ZmOSCA family members involved in osmotic stress and *ZmOSCA2.4* confers enhanced drought tolerance in transgenic *Arabidopsis*. *Int. J. Mol. Sci.* **2020**, *21*, 351. [CrossRef] [PubMed]
15. Miao, S.; Li, F.; Han, Y.; Yao, Z.; Xu, Z.; Chen, X.; Liu, J.; Zhang, Y.; Wang, A. Identification of OSCA gene family in *Solanum habrochaites* and its function analysis under stress. *BMC Genom.* **2022**, *23*, 547. [CrossRef]
16. Li, J.; Yang, J.; Jia, B. Evolution and expression analysis of OSCA gene family in soybean. *Chin. J. Oil Crop Sci.* **2017**, *16*, 16–26.
17. Cao, Y.; Feng, J.; Hwarari, D.; Ahmad, B.; Wu, H.; Chen, J.; Yang, L. Alterations in population distribution of *Liriodendron chinense* (Hemsl.) Sarg. and *Liriodendron tulipifera* Linn. caused by climate change. *Forests* **2022**, *13*, 488. [CrossRef]
18. Chen, J.; Hao, Z.; Guang, X.; Zhao, C.; Wang, P.; Xue, L.; Zhu, Q.; Yang, L.; Sheng, Y.; Zhou, Y.; et al. Liriodendron genome sheds light on angiosperm phylogeny and species-pair differentiation. *Nat. Plants* **2019**, *5*, 18–25. [CrossRef]
19. Zhao, K.; Chen, S.; Yao, W.; Cheng, Z.; Zhou, B.; Jiang, T. Genome-wide analysis and expression profile of the bZIP gene family in poplar. *BMC Plant Biol.* **2021**, *21*, 122. [CrossRef]
20. Hwarari, D.; Guan, Y.; Li, R.; Movahedi, A.; Chen, J.; Yang, L. Comprehensive bioinformatics and expression analysis of TCP transcription factors in *Liriodendron chinense* reveals putative abiotic stress regulatory roles. *Forests* **2022**, *13*, 1401. [CrossRef]
21. Wu, W.; Zhu, S.; Xu, L.; Zhu, L.; Wang, D.; Liu, Y.; Liu, S.; Hao, Z.; Lu, Y.; Yang, L.; et al. Genome-wide identification of the *Liriodendron chinense* WRKY gene family and its diverse roles in response to multiple abiotic stress. *BMC Plant Biol.* **2022**, *22*, 25. [CrossRef] [PubMed]
22. Li, R.; Radani, Y.; Ahmad, B.; Movahedi, A.; Yang, L. Identification and characteristics of SnRK genes and cold stress-induced expression profiles in *Liriodendron chinense*. *BMC Genom.* **2022**, *23*, 708. [CrossRef] [PubMed]
23. Subramanian, B.; Gao, S.; Lercher, M.J.; Hu, S.; Chen, W.H. Evolview v3: A webserver for visualization, annotation, and management of phylogenetic trees. *Nucleic Acids Res.* **2019**, *47*, W270–W275. [CrossRef] [PubMed]
24. Procter, J.; Carstairs, G.; Soares, B.; Mourao, K.; Ofoegbu, T.; Barton, D.; Lui, L.; Menard, A.; Sherstnev, N.; Roldan-Martinez, D.; et al. Alignment of biological sequences with Jalview. *Methods Mol. Biol.* **2021**, *2231*, 203–224.
25. Li, M.; Hwarari, D.; Li, Y.; Ahmad, B.; Min, T.; Zhang, W.; Wang, J.; Yang, L. The bZIP transcription factors in *Liriodendron chinense*: Genome-wide recognition, characteristics and cold stress response. *Front. Plant Sci.* **2022**, *13*, 1035627.
26. Chen, C.; Chen, H.; Zhang, Y.; Thomas, H.R.; Frank, M.H.; He, Y.; Xia, R. TBtools: An integrative toolkit developed for interactive analyses of big biological data. *Mol. Plant* **2020**, *13*, 1194–1202. [CrossRef]
27. Pan, G.; Li, Z.; Yin, M.; Huang, S.; Tao, J.; Chen, A.; Li, J.; Tang, H.; Chang, L.; Deng, Y.; et al. Genome-wide identification, expression, and sequence analysis of CONSTANS-like gene family in cannabis reveals a potential role in plant flowering time regulation. *BMC Plant Biol.* **2021**, *21*, 142. [CrossRef]
28. Yu, C.; Ke, Y.; Qin, J.; Huang, Y.; Zhao, Y.; Liu, Y.; Wei, H.; Liu, G.; Lian, B.; Chen, Y.; et al. Genome-wide identification of calcineurin B-like protein-interacting protein kinase gene family reveals members participating in abiotic stress in the ornamental woody plant *Lagerstroemia indica*. *Front. Plant Sci.* **2022**, *13*, 942217. [CrossRef]
29. Li, R.; Ahmad, B.; Hwarari, D.; Li, D.; Lu, Y.; Gao, M.; Chen, J.; Yang, L. Genomic survey and cold-induced expression patterns of bHLH transcription factors in *Liriodendron chinense* (Hemsl) Sarg. *Forests* **2022**, *13*, 518. [CrossRef]
30. Ding, S.; Feng, X.; Du, H.; Wang, H. Genome-wide analysis of maize OSCA family members and their involvement in drought stress. *PeerJ* **2019**, *7*, e6765. [CrossRef]

31. Yang, X.; Xu, Y.; Yang, F.; Magwanga, R.O.; Cai, X.; Wang, X.; Wang, Y.; Hou, Y.; Wang, K.; Liu, F.; et al. Genome-wide identification of OSCA gene family and their potential function in the regulation of dehydration and salt stress in *Gossypium hirsutum*. *J. Cotton Res.* **2019**, *2*, 11. [CrossRef]
32. De Zelicourt, A.; Colcombet, J.; Hirt, H. The role of MAPK modules and ABA during abiotic stress signaling. *Trends Plant Sci.* **2016**, *21*, 677–685. [CrossRef] [PubMed]
33. Bulgakov, V.P.; Wu, H.C.; Jinn, T.L. Coordination of ABA and chaperone signaling in plant stress responses. *Trends Plant Sci.* **2019**, *24*, 636–651. [CrossRef] [PubMed]
34. Hussain, Q.; Asim, M.; Zhang, R.; Khan, R.; Farooq, S.; Wu, J. Transcription factors interact with ABA through gene expression and signaling pathways to mitigate drought and salinity stress. *Biomolecules* **2021**, *11*, 1159. [CrossRef] [PubMed]
35. Colebrook, E.H.; Thomas, S.G.; Phillips, A.L.; Hedden, P. The role of gibberellin signalling in plant responses to abiotic stress. *J. Exp. Biol.* **2014**, *217*, 67–75. [CrossRef]
36. Wang, J.; Liu, Y.; Tang, B.; Dai, X.; Xie, L.; Liu, F.; Zou, X. Genome-wide identification and capsaicinoid biosynthesis-related expression analysis of the R2R3-MYB gene family in *Capsicum annuum* L. *Front Genet.* **2020**, *11*, 598183. [CrossRef]
37. Han, Y.; Wang, Y.; Zhai, Y.; Wen, Z.; Liu, J.; Xi, C.; Zhao, H.; Wang, Y.; Han, S. OsOSCA1.1 mediates hyperosmolality and salt stress sensing in *Oryza sativa*. *Biology* **2022**, *11*, 678. [CrossRef]
38. Min, T.; Hwarari, D.; Li, D.; Movahedi, A.; Yang, L. CRISPR-based genome editing and its applications in woody plants. *Int. J. Mol. Sci.* **2022**, *23*, 10175. [CrossRef]